3

Proximal Records of Paleotsunami Runup in Barrage Creek Floodplains from Late-Holocene Great Earthquakes in the Central Cascadia Suduction Zone, Oregon, USA

Curt D. Peterson and Kenneth M. Cruikshank
Department of Geology, Portland State University, Portland, OR, USA

1. Introduction

A 100 km section of the central Oregon coast (Fig. 1) was surveyed for proximal creek floodplains, located at less than 500 m distance from the ocean shoreline, that could host sand sheet records of paleotsunami inundation (Peterson & Cruikshank, 2007). The study region is located near the center of the Cascadia margin, an active subduction zone that spans about 1000 km distance in the central west coast of North America (Atwater et al., 1995; Darienzo et al., 1994). Previous work in two distal floodplain localities within the study region, Neskowin and Beaver Creek, showed multiple paleotsunami inundations of one to several kilometers distance landward during the last ~ 2,500 years (see section 2.2) (Peterson et al., 2010a). It was not known how those distal records might relate to proximal or shoreline runup heights of the same paleotsunami events in the region. Such proximal or near-shoreline runup heights are needed to 1) demonstrate flooding hazards in coastal areas that have not suffered catastrophic flooding in historic time (Dengler, 2006), and 2) independently test flooding predictions based on assumed fault displacements and numerical tsunami runup models (González et al., 2009).

In this paper we document anomalous sand sheet layers in 8 small creek floodplains that exceed 6 m elevation thresholds for tsunami inundation. Target sand sheets are examined for evidence of marine shell fragments, tracers of marine surge origins, and the landward limits of sand sheet extent. The time span of continuous deposition in one representative floodplain locality is dated by radiocarbon. An adjacent floodplain locality is examined for landward trends of sand sheet composition, sand sheet thickness, microscopic tracers of marine deposits, and sand sheet radiocarbon age. Maximum sand sheet extent in the proximal floodplain locality is compared to maximum sand sheet extent in a distal floodplain locality (Peterson et al., 2010a) to yield a landward runup height gradient for the most recent event of large magnitude runup. The runup attenuation gradient is tested against previously reported runup elevations in another central Cascadia study area, Cannon Beach, Oregon (Fig. 1) (Peterson et al., 2008). The methods reported here should be applicable in similar settings to the documentation of paleotsunami runup heights in other susceptible coastlines around the world.

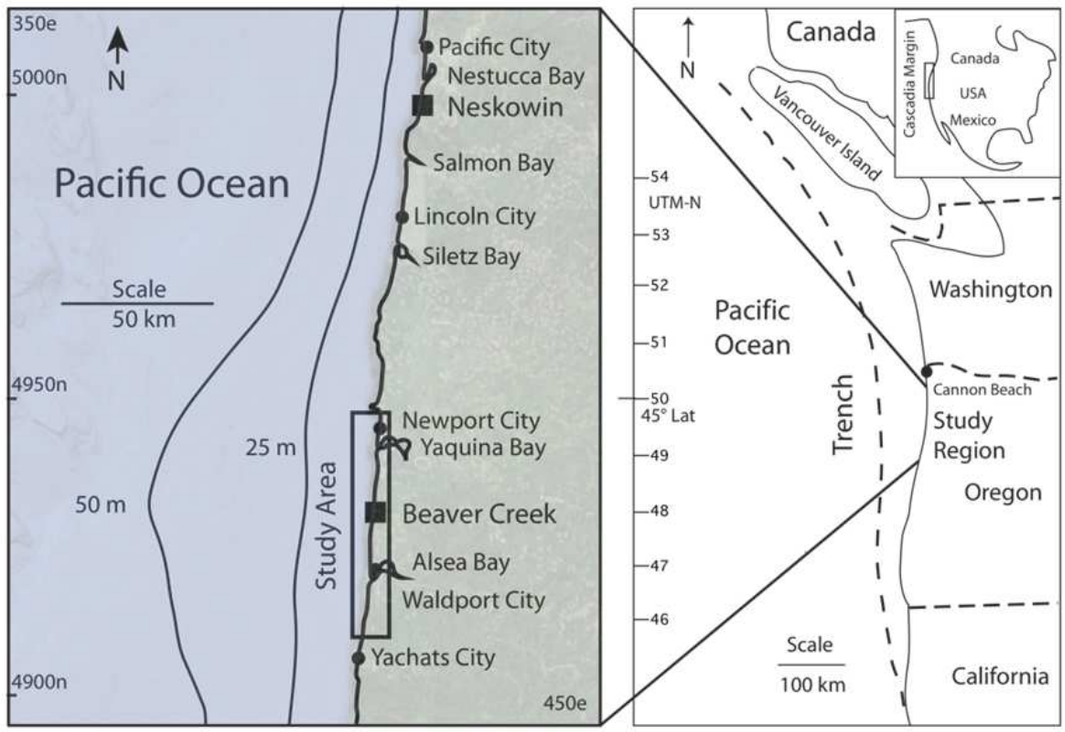

Fig. 1. The paleotsunami study region (~ 100 km in length) is located in the central Cascadia subduction zone (map at right). The Cascadia megathrust daylights along the trench (dashed line). The focused study area (~ 35 km in length) is shown in central Oregon coast (boxed area in inset map at left). Coastal communities (solid circles) and small estuaries (Bays) are named. Two localities investigated for paleotsunami inundation in distal floodplain settings are shown at Neskowin and Beaver Creeks (solid squares). Map coordinates for the study region (inset map at left) are in UTM x 1,000 m. Basemap is from Google (2011).

2. Study region

2.1 Paleoseismic evidence

A total of six or seven great earthquakes that ruptured though the central Cascadia margin during the last ~ 3,000 years are well recorded in Washington and northernmost Oregon where coseismic subsidence of least 1.0 m predominates (Table 1). Investigations of the associated nearfield paleotsunami inundations moved from the coastal marshes to overland inundation recorded in lakes, beach plains, back-barrier wetlands, and barrage lakes (Hutchinson et al., 1997; Kelsey et al., 2005; Schlichting & Peterson, 2006). The geologic records of paleotsunami sand sheet deposition that are located landward of foredunes, beach ridges, and other unstable coastal barriers provide minimum estimates of runup height (Peterson et al., 2006). To overcome these limitations some recent investigations have been redirected towards mapping paleotsunami sand sheets in small alluvial floodplains that are located on relative stable marine terraces (see Section 2.2 below).

Event	Atwater	Tsunami #	Age
Subsidence / Tsunami	Y	1	0.3 (AD1700)
? / Tsunami	-	2a	~ 0.9
Subsidence / Tsunami	W	2b	~ 1.1
Subsidence / Tsunami	U	3	~ 1.3
Subsidence / Tsunami	S	4	~ 1.7
Subsidence / Tsunami	H	5	~ 2.6
Subsidence / Tsunami	L	-	~ 2.8
Subsidence / ?	J	-	~ 3.2

Table 1. Central Cascadia Margin rupture and tsunami events. Subsidence related rupture events and ages are from Atwater et al., (2004). Tsunami correlations (Tsunami #) in the central Cascadia margin are from Peterson et al., (2010a). The source of the 2nd tsunami sand layer in the central Cascadia tsunami is not known (Peterson et al., 2008), but it might reflect a partial rupture in the northern part of the Cascadia margin (Clague et al., 2000; Schlichting & Peterson, 2006). Due to difficulties of discriminating the 2nd and 3rd tsunami events in some floodplain settings we assign them numbers of #2a and #2b, where they can be discriminated, and #2 where only one layer can be discriminated. Tsunami inundation has yet to be verified in the study area for the rupture events L and J at ~ 2.8 and 3.2 ka, respectively.

2.2 Distal paleotsunami runup records

Paleotsunami records have been reported from two alluvial floodplain settings in the central Oregon coast, Neskowin and Beaver Creek (Fig. 1)(Table 2) (Peterson et al., 2010a). The two localities differ in landward floodplain gradient and protective barrier ridges. A low-gradient floodplain (0 to 3 m elevation) in the Beaver Creek Valley records landward thinning sand sheets (20 to 1 cm thickness) over inundation distances of 1 to 4 km from the beach. In this paper all reported elevations are in the NAVD88 datum, which is about 1 meter below mean sea level (MSL).

The two longest paleotsunami runups in Beaver Creek correspond to dated paleotsunami deposits at 1520-1700 BP and 2960-3220 BP (Table 2). The age of the tsunami remobilized organic debris should predate the Cascadia rupture event, so we assign the two events to tsunami #3 and tsunami #5 or #6. The oldest three rupture events (H, J, and L) have short recurrence intervals (Table 1), so the radiocarbon ages of their associated tsunami deposits might overlap.

The Neskowin back-barrier wetlands are fronted by a barrier dune ridge (5–8 m elevation) and are backed by an uplifted terrace, which is dissected by small creeks. Sand sheets from four nearfield paleotsunami were traced across the back-barrier wetland (3 m elevation) and into a high-gradient creek floodplain, Hawk Creek, at elevations of 3 to 8 m at distances of ~ 0.5 to 1.0 km from the ocean shoreline (Table 2). The longest and highest tsunami runup at Neskowin, dated at 1114-1300 BP, is correlated to tsunami #3, which is coincident with the youngest of the two longest runup events in Beaver Creek.

3. Methods

The central Oregon coast was selected for this study based on a straight coastline, with low marine terraces that are dissected my numerous small creek valleys. Gouge coring (2.5 cm

Distal Record Locality	Rupture Age (ka)	TSL event (#)	Max. TSL thickness (cm)	Pinchout distance (km)	Terminal elevation (m, NAVD88)	Calibrated Radiocarbon (yr BP ± 2 σ)
Beaver Ck	0.3	1	20	2.5	0.0	320-520
	0.9	2a	8	0.5-1.0	0.0	
	1.1	2b	12	1.5	0.0	
	1.3	3	16	4.1	1.5	1520-1700
	1.7	4	5	1.5-2.0	0.0	
	2.6-2.8	5-6	6	4.0	0.7	2960-3220
Neskowin	0.3	1	20	0.6	3.0	-
	0.8	2a	5	0.6	3.0	-
	1.1	2b	8	0.8	6.5	940-1140
	1.3	3	40	1.0	8.3	1140-1300

Table 2. Overland paleotsunami runup records in distal alluvial flood plain settings, central Oregon coast. Rupture ages for the central Cascadia margin are from Atwater et al., (2004). Neskowin and North Beaver Creek data are from Peterson et al., (2010a) and Schlichting (2000). Distances from the ocean shoreline (km) are based on observed tsunami sand deposition, so they might underestimate maximum flooding distance. Elevations of terminal deposits (m NAVD88) shown here are not adjusted for late Holocene rise of sea level height. A net relative sea-level rise of 1m/1000 yr can be applied to the older paleotsunami events to correct for increased runup heights at the time of inundation. Radiocarbon ages (calibrated at ±2 sig. yr BP) are based on transported tsunami debris, so they should predate the corresponding rupture event age. Beaver Creek and Neskowin Creek floodplain localities are shown in Fig. 1.

diameter x 2.0 m core lengths) and/or ram coring (7.5 cm diameter x 2.0 m core lengths) were used to test the creek floodplain deposits for anomalous landward-thinning sand sheets. The surveyed core sites were investigated with 2 to 5 core retrievals prior to 1) core photography (50 mm macro-lens on a 10 megapixel DSLR), 2) subsampling for sand size, carbonate shell fragments, diatoms, and radiocarbon dating, and 3) logging at the 1 cm length scale. Core site positions are established by 12 channel WAAS-enabled GPS (e.p.e. 2.5-5.0 m). Locality elevations are taken from LiDAR (U. S. Geological Survey, 2011). Selected core sites are surveyed into registered benchmarks by EDM-Total Station for precise elevation control (elevation error ± 5 cm). Photos of target tsunami deposits, site position data, elevation surveying data, and initial field logs are archived in the Oregon Tsunami Database (Cruikshank & Peterson, 2011)

In the previous studies of paleotsunami runup in distal alluvial floodplains (see Section 2.2) heavy mineral tracers were used discriminate between beach sand and river sand sources to the target paleotsunami sand sheets (Peterson et al., 2010a). That approach could not be used in the proximal alluvial floodplains, due the presence of uplifted Pleistocene beach and dune deposits in the small alluvial drainages, which could contribute beach sand minerals to the creek sand bedload. The presence of marine diatoms has previously been used to establish paleotsunami inundation in some upland or inland freshwater settings of the Cascadia margin (Hemphill-Haley, 1996; Hutchinson

et al., 1997; Kelsey et al., 2005). However, unexpected traces of marine diatoms in some control intervals, or non-tsunami deposits, from the central Cascadia beach plains and floodplains have suggested marine diatom transport by ocean wind/spray to distances of 2 km inland from the beach (Peterson et al., 2010a; Schlichting & Peterson, 2006). To further test these findings some target paleotsunami deposits and control intervals in the creek floodplains were examined for diatom taxa abundances following methods provided by Schilchting (2000).

Carbonate shell fragments provide an alternative marine source tracer for the target paleotsunami sand layers in proximal localities where the presence of small gravel size fractions (> 2 mm diameter) include marine shell fragments. Shell fragments in the granule and small pebble size ranges can usually be identified in the field with hand lens and 7.0 molar HCL for dissolution testing.

Another technique for indentifying carbonate shell fragments was used for the finer sand size fractions in the more landward sites of the proximal localities. Small carbonate fragments (0.2-0.5 mm diameter) in the sand size fraction are present at trace abundances (1,000 total grain counts per sample). They are identified in grain mounts by moderately high relief and high dispersion in polarized light under petrographic microscopy at 250x.

Sediment grain sizes are analyzed in the target paleotsunami deposits to establish any vertical trends and landward trends in grain size distributions. Upward grain-size fining trends are established by high-resolution digital photography at ~ 50x magnification. Landward fining trends are based on petrographic microscopy (250x) of grain counts (50 total grains per slide) of samples taken from the middle of target tsunami sand layers. Standard statistical methods for characterizing the sample grain size populations follow Folk (1980).

Samples of organic detritus, including leaves and twigs, were collected from tsunami sand sheet layers for radiocarbon dating by AMS method. Small samples (< 0.5 g) were air dried, weighed and submitted to Beta Analytic Inc. for dating. Sample dates are provided in isotope adjusted radiocarbon age and in calibrated radiocarbon years BP at the 2–σ analytical error level by Beta Analytic Inc.

3.1 High-gradient proximal floodplains

In this study we target high-gradient floodplains in the central Oregon coast for sand sheet records of proximal paleotsunami runup (Fig. 2; Table 3). The small creek floodplains rise from 5 m to as much as 15 m in elevation within short distances (0.5-1.0 km) from the beach. The incised creek valleys were downcut into Pleistocene dune sheets and underlying marine terraces during the last sea level lowstand. The perched creek floodplains formed after late-Holocene beach sand ramped against the sea cliffs and creek mouths in the study area (Hart & Peterson, 2007). The onset of surplus beach sand supply began between 4.0 and 4.5 ka based on dated buried stumps on the beach platform at Grant Creek and Deer Creek, and from a sea cliff dune ramp at Lost Creek (Fig. 2; Table 3). The excess supply of beach sand slowed or stopped by about 3.0 ka in the study area, based on a radiocarbon date from the top of the dune ramp that blocked Quail Creek. Seasonal flooding and shallow groundwater surfaces in the creek valleys permitted accumulations of peaty mud in the floodplains, which serve as hosting deposits for landward thinning layers of beach sand.

4. Results

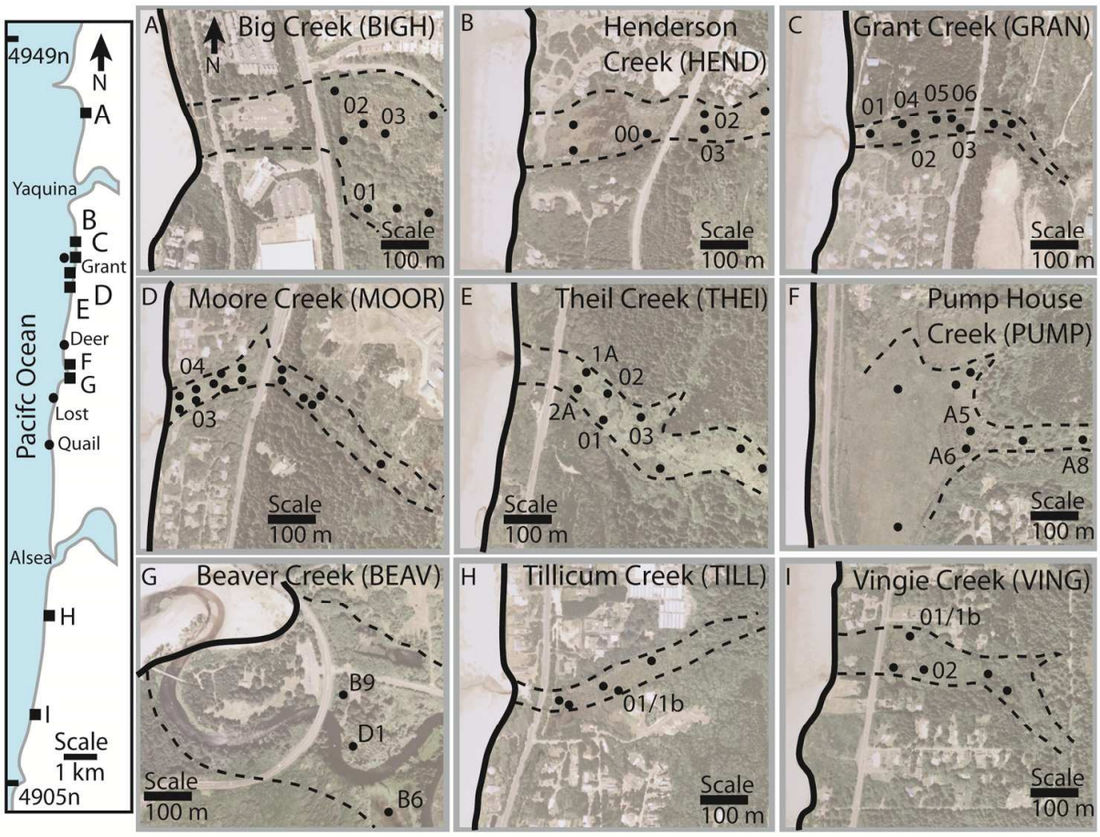

Fig. 2. Study area includes 9 creek floodplain localities (maps), and buried beach platform stumps or dune ramp forest soils at Grant Creek, Deer Creek, Lost Creek, and Quail Creek. Beach platform and dune ramp radiocarbon dates are shown in Table 4. Representative core sites are summarized in Table 3. Core logs and core site position data are provided in Cruikshank and Peterson (2011).

4.1 Paleotsunami records in proximal high-gradient alluvial wetlands

Eight proximal runup localities with inundation thresholds of 6.0 to 7.5 m elevation (NAVD88) in the study area are found to contain multiple anomalous sand sheets in creek floodplain deposits (Table 3). Alluvial mud hosts the anomalous sand sheets, which fine upward and thin landward in the small floodplain settings (Fig. 3). Additional creek floodplains exist within the 100 km long study region, but the tight grouping of eight localities within a 35 km study area permits comparisons of different catchment responses to similar conditions of tsunami surge forcing. The southern grouping of alluvial creek wetlands is divided on either side of the low gradient Beaver Creek valley that contains the longest overland inundation records reported to date for the central Cascadia margin (Table 2).

Six out of the eight creek localities record three or four prominent sand sheets, suggesting a similarity in age span of the alluvial hosting deposits. Radiocarbon dating of the alluvial section in Grant Creek, containing three sand sheets and one sandy debris layer, yields an age range from post-modern carbon (107pmc) to 3480-3690 BP (Table 4). The age span for

Locality/ Core Sites	UTM Northing (m)	UTM Easting (m)	Shoreline distance (m)	Threshold /core elev. (m)	TSL number	TSL max. thickness (cm)
BIGC2/3	4945660	416690	400	6.5/6.5	2	7
HEND3/4	4938210	415680	420	6.0/5.5	3	12
GRAN5/6	4936930	415250	120	6.0/8.0	3	10
MOOR3/4	4936080	415140	80	7.5/8.0	3	36
THEI1A/2	4935090	415110	100	6.0/5.5	3	12
PUMP5/6	4931050	414870	340	6.0/6.5	3	12
BEAV_D1	4930160	414990	400	4.5/2	4	13
TILL1/1b	4916010	413630	250	6.0/5.5	2	5
VING1/1b	4910390	412680	170	6.0/7.0	3	5

Table 3. Representative proximal runup core sites in the central Oregon coast. Core site elevation is based on core site surface elevations (m, NAVD88) taken from LiDAR (U. S. Geological Survey, 2011). Distance is the straight-line distance (m) of surge flow from beach backshore or sea cliff to the representative core sites. Threshold elevation (m, NAVD88) is based on the mean across-valley elevation at or near the shoreline. TSL number is the number of observed tsunami sand layers of least 1 cm sand thickness in each runup locality. TSL maximum thickness is the thickest target tsunami sand layer (cm) observed in the runup locality. Core sites in creek floodplain localities are shown in Fig. 2. Data from Cruikshank and Peterson (2011).

the Grant Creek silt alluvium, located just above basal creek gravel, is consistent with an expected onset of creek damming by dune ramp barrages that occurred at about 4 ka in the study area (see Section 4.1).

The tsunami sand layers (TSL) decrease in number and thickness with increasing landward distance and elevation in each runup locality (Fig. 2). The tsunami sand layers fine upward, terminating with thin laminae of very-fine sand or silt at the tops of the sandy intervals (Fig. 3). Sandy organic debris layers (TDL), which commonly cap tsunami sand sheets in distal alluvial runup localities of the Cascadia margin (Carver et al., 1998; Peterson et al., 2008), are uncommon in the proximal runup localities observed in the central Oregon study area. These data demonstrate that as many as four paleotsunami inundations substantially overtopped the barrage dune barriers (6.0 to 7.5 m elevation) at the mouths of corresponding creeks during the last several thousand years.

Site	Setting	adjC14 yr ± error	Cal RC 2-σ (yr BP)	Lab
Grant Creek beach	Beach platform stump	3750±60	3988-4228	B118658
Lost Creek beach	Beach dune ramp	3420±60	3600-3720	B148094
Deer Creek beach	Beach platform stump	3920±60	4255-4421	B81340
Quail Creek mouth	Top of barrage dune	2930±40	3018-3152	B172772

Table 4. Radiocarbon dates for dune ramps and creek barrage dunes in the study area. Data for Grant Creek beach platform stump (UTM 4936010n 415050e), Lost Creek beach dune ramp (UTM 4933080n 414770e), Deer Creek beach platform stump (UTM 4928880n 414110e, and Quail Creek top of barrage dune (UTM 4926060n 413880e) are from (Hart & Peterson, 2007). The dated sites of buried beach platform stumps and sea cliff dune ramps are shown in Fig. 2.

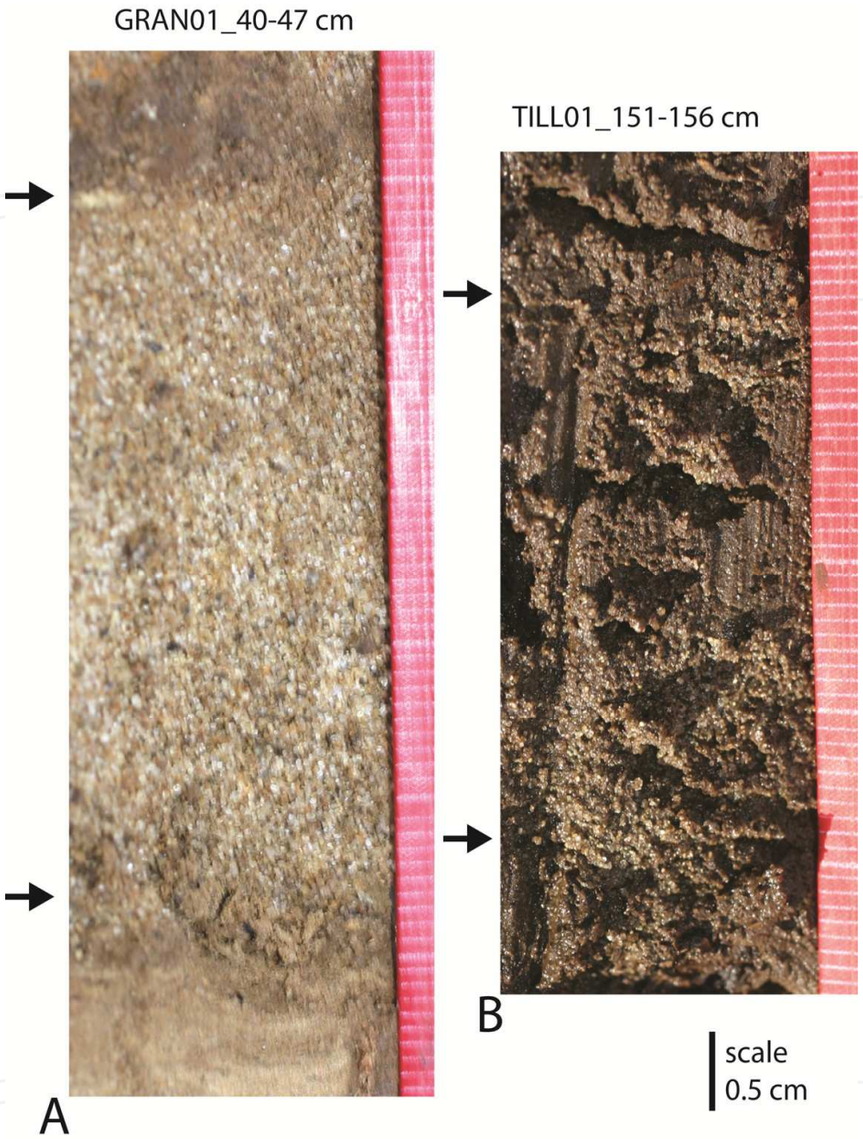

Fig. 3. Contrasting paleotsunami sand layers shown between black arrows for (A) Grant Creek (40-47 cm depth at core site GRAN1) and (B) Tillicum Creek (151-156 cm depth at core site TILL1). The sand sheet deposit from Grant Creek (5-6 cm thick) shows 1) an undisturbed tsunami sand layer (TSL), 2) clear contrast with oxidized hosting alluvium, 3) a sharp bottom contact, 4) fining-upward grain-size trend, and 5) a dark organic-rich debris layer (TDL). The sand sheet deposit from Tillicum Creek (~ 3-4 cm thick) is much disturbed by root bioturbation and the quartz-rich beach sand is obscured by the dark reducing hosting mud. However it does have a sharp lower contact, and it fines upward in grain-size, though no capping debris layer is apparent. Red tape rule is scaled at 1 mm intervals. See Fig. 2 for core site locations.

Several recent paleotsunami with limited inundations in distal runup localities, Neskowin and Beaver Creek, include the last three central Cascadia tsunami events TSL #1, #2a and #2b, (Table 3). Paleotsunami events with expected low runup heights, including events #1 and #2a, are recorded in the low elevation wetlands at the mouth of Beaver Creek in core site BEAV_D1 (Fig. 4). These lower runup events did broadly overtop minimum threshold elevations of the beach backshore at 4.5 m elevation that fronts the mouth of Beaver Creek (Fig. 2). Based on these minimum threshold elevations of recorded paleotsunami inundation we estimate minimum runup heights of at least 5.0 m for nearfield tsunami in the central Cascadia margin.

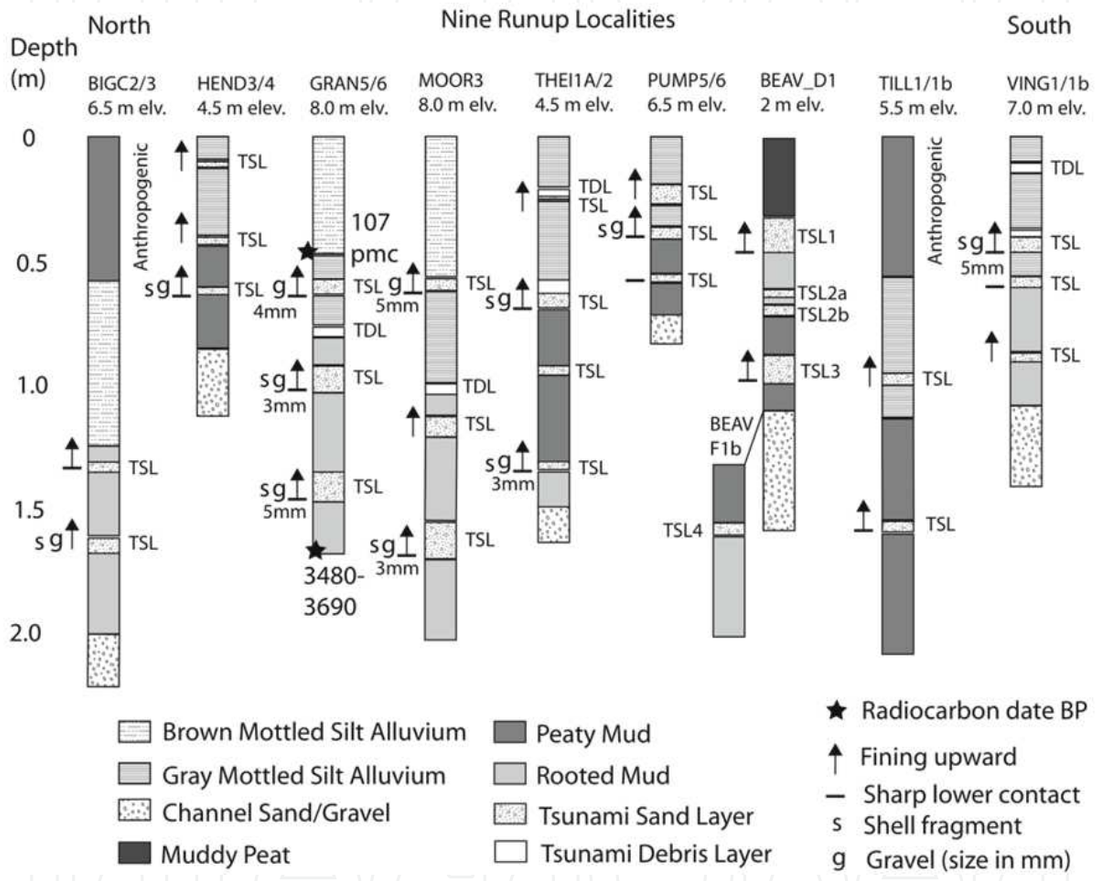

Fig. 4. Representative core logs from nine creek runup localities in the central Oregon coast study area, including Big Creek (BIGC), Henderson Creek (HEND), Grant Creek (GRAN), Moore Creek (MOOR), Theil Creek (THEI), Pumphouse Creek (PUMP), Beaver Creek (BEAV), Tillicum Creek (TILL), and Vingie Creek (VING). Target tsunami layers are verified in two adjacent core sites from each elevated floodplain, except Moore Creek, where additional core logs are shown in later sections of the paper. The position data for the localities and corresponding core sites are shown in Fig. 2 and Table 3. Core site elevations (m) are relative to the NAVD88 datum. One proximal locality (BEAV_D1) is a low elevation back-barrier wetland, whereas the other eight creek floodplain localities all exceed 6 m elevations at their shoreline barrage-dune thresholds.

Three runup localities in the study area, including Grant, Moore, Theil, and Vingie Creeks, contain anomalous sandy silt layers that can be correlated between successive target

tsunami sand layers in adjacent core sites (Cruikshank & Peterson, 2011). Such isolated tsunami debris layers (TDL) are shown in core sites GRAN5/6 and MOOR3 (Fig. 4). These layers might represent terminal inundations by smaller tsunami events. Other smaller target layers (< 1 cm thickness) might exist in the seaward sites of the study area localities, but are not further addressed in this study.

Locality/ Site	Depth (cm)	adjC14 yr ± error	Cal RC 2-σ (yr BP)	Lab
GRAN6_54	54	107±0.5pMC	modern	B281145
GRAN6_161	161	3360±40	3,480-3,690	B281146
MOOR9_86	86	1,830±40	1,640-1,650	B230659
MOOR9_120	120	2,720±40	2,750-2,880	B228599
MOOR9_129	128.5	2940±40	2,960-3,230	B222512
MOO9-200	200	3,390±40	3,560-3,710	B228600

Table 5. Radiocarbon dates for paleotsunami in proximal runup sites, central Oregon coast. Radiocarbon dates are taken from base of tsunami sand layers, as shown by core depth (cm). See Fig. 2 for core sites and Fig. 4 and Fig. 7 for core logs.

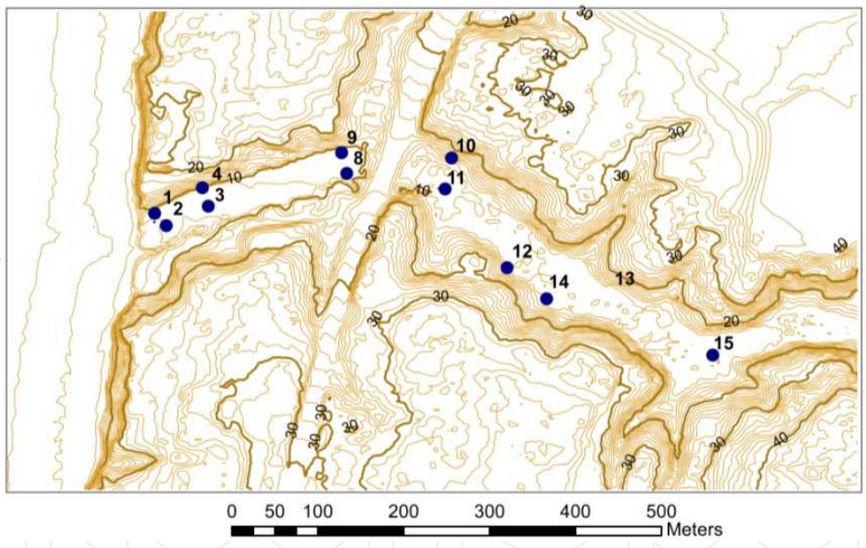

Fig. 5. Moore Creek core site map including 12 representative core sites ranging from 8 to 13 m in elevation (NAVD88). Contour base map is based on LIDAR DEM (U. S. Geological Survey, 2011). 1m contour interval, with bold contours at 10, 20, and 30 m elevation. See Fig. 2 for location of Moore Creek locality in the study area. Core photos and core logs are shown in Fig. 6 and Fig. 7, respectively.

Though flow height and duration are both important in surge magnitude, for this study we focus on estimating runup height in the proximal floodplain settings. To establish maximum-recorded runup elevations the tsunami sand sheets are traced to their most landward extent in several creek localities. The terminal sand sheet deposits that show the best preservation and continuity occur in the Moore Creek floodplain locality (Fig. 2).

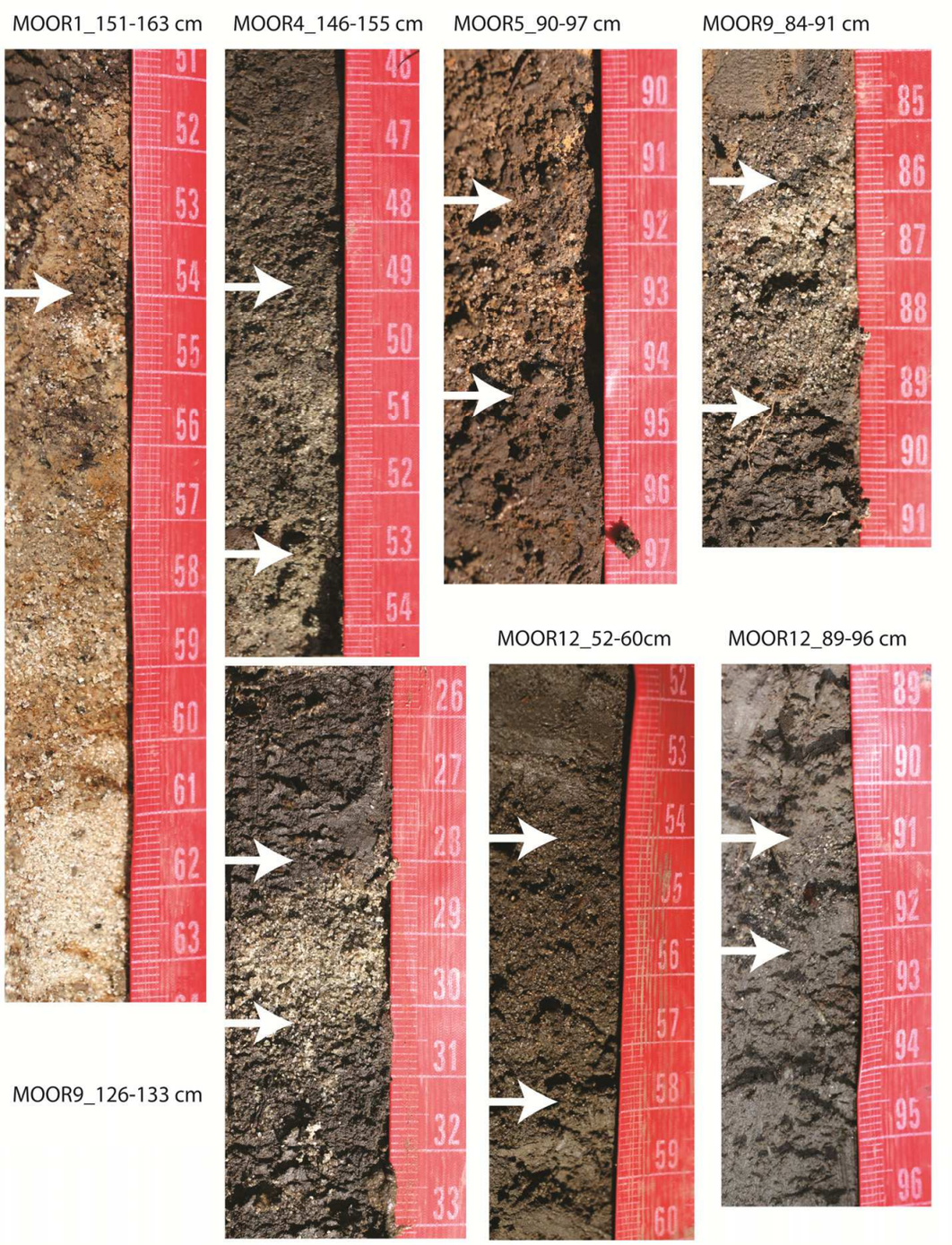

Fig. 6. Photos of representative tsunami sand layers (TSL) from the Moore Creek locality. Core sections are listed by core site number and depth (cm). Tsunami sand layers are bracketed by white arrows. The tsunami sand layer in MOOR01 continues 154–163 cm depth in the photo to 187 cm depth below the photo, totaling 33 cm in thickness. The thin sandy layer in MOOR12 at 91-92 cm depth is transitional between a tsunami sand layer and sandy tsunami debris layer. See Fig. 7 for core logs.

4.2 Moore creek runup locality

A total of 12 representative core sites are logged to document the landward thinning of sand sheets hosted in alluvial silts of the Moore Creek locality (Fig. 5). The sand sheets thin to only a few centimeters in thickness with increasing landward distance and elevation gain in the high-gradient floodplain setting. However, the quartz-rich beach sand layers are distinctive in the gray silt alluvium (Fig. 6).

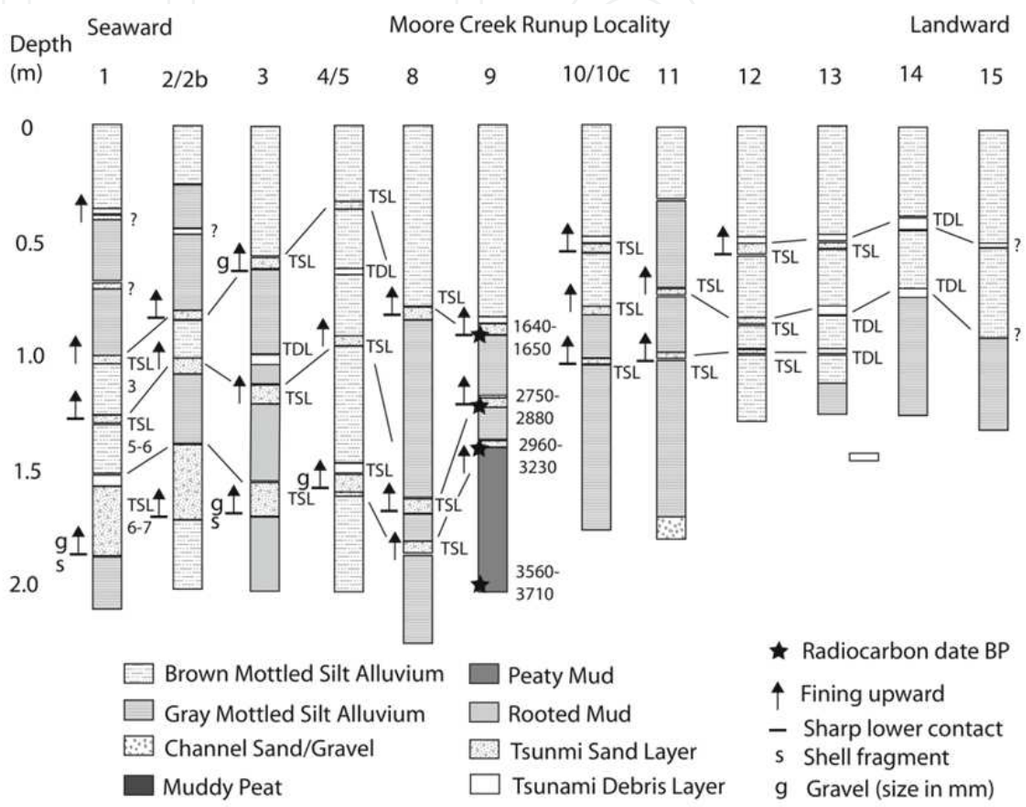

Fig. 7. Core Logs from the Moore Creek runup locality showing tsunami sand layers (TSL) and tsunami debris layers (TDL) in representative core sites. See Fig. 5 for core site positions and Table 8 for core site elevations.

The three sand sheets that largely span the length of the Moore Creek runup locality are dated by AMS radiocarbon analyses of organic debris in the base of the sand sheets in core site MOOR9 (Fig. 7**;** Table 4). The radiocarbon samples yield dates of 1640–1650 BP, 2750–2880 BP, and 2960–3230 BP, corresponding to Cascadia tsunami events #3, #5, and #6–7, respectively (Table 1). A radiocarbon date of 3560–3710 BP dates the onset of alluvial silt accumulation in the Moore Creek floodplain at site MOOR9. Several anomalous sand laminae (< 1 cm thickness) are apparent above or between the prominent sand sheets in the seaward core sites MOOR1, MOOR2, MOOR3 and MOOR4. The origins of these minor lamiane are not known, but could reflect terminal deposits of smaller runup events. Due to their lack of continuity in the landward core sites they are not further addressed in this paper.

Three depositional features are common in the three target tsunami deposit layers from the Moore Creek core sites, including sharp lower contacts, sediment fining-upward trends, and

deposit layer thinning with increasing distance landward (Fig. 7). The combination of all three features in the three target sand layers is consistent with catastrophic marine surges but not with river flooding, paleoliquefaction, or hillslope debris flows. Further tests of marine surge origin are provided by marine source tracers in the target tsunami sand sheets (see Section 4.4 below).

4.3 Marine surge tracers

The use of marine diatoms to confirm paleotsunami inundation in the proximal flood plain settings that were investigated in this study proved to be problematic. Diatoms occur in the silt size range, and are potentially very useful in discriminating marine surge sources of target paleotsunami layers in the Cascadia margin (Hemphill-Haley, 1996; Kelsey et al., 2005; Schlichting & Peterson, 2006). In this study a composite sample was taken from the top of the target tsunami layer where the fine to very-fine sand in the tsunami sand layer grades into sandy silt or sandy detrital organics in the tsunami debris layer. Ocean derived diatoms including full marine and brackish taxa are present in the paleotsunami layers from the Moore Creek locality (Table 6). As expected, diagnostic freshwater diatoms are also present in the flood plain soils. Diagnostic ocean derived diatoms are also present in very-low abundance in control intervals are that are not associated with target paleotsunami sand layers or paleotsunami debris layers in the Moore Creek locality. The presence of marine and brackish diatoms in trace to minor abundances in non-tsunami control layers, argues for ocean diatom transport in wind driven ocean foam and/or spray in proximal settings (100-400 m from the beach). Additional evidence is needed to confirm the marine surge origins of the target paleotsunami sand sheets in the proximal floodplain settings.

Diatom Assemblage/ Taxa	Core Site	Depth (cm)	Target layer
Polyhalobous (marine)			
Hyalodiscus scoticus	MOOR9	55-60	control
Coscinodiscus radiatus	MOOR12	54-58	TSL/TDL
Cocconeis scutellum	MOOR12	54-58	TSL/TDL
Endycta sp.	MOOR12	100-101	control
Mesohalobous (brackish)			
Navicula lanceola	MOOR9	86-88	TSL
Pinnularia viridis	MOOR9	119-122	TSL
Pinnularia viridis	MOOR12	128-130	TSL/TDL
Opephora parva	MOOR12	128-130	TSL/TDL
Oligohalobous (freshwater)	MOOR9, 12		
Amphora ovalis	MOOR9, 12		
Eunotia pectinal	MOOR9, 12		
Gomphonema parvulum	MOOR9, 12		

Table 6. Presence of diagnostic diatom taxa in proximal alluvial deposits. Control layers are non-tsunami layers. TSL are target paleotsunami sand layers. TDL are target paleotsunami debris layers. Core sites and sample intervals are shown in Fig. 5 and Fig. 7, respectively.

	TSL number	Max. size (μm)	Min. size (μm)	Mean Size (μm)	Std Dev +/- (μm)	MeanN StdDev	Shell frag (%)
Beach		460	180	269	56	0.21	0.27
Creek		1030	150	470	234	0.50	0.00
1_100 cm	#3	610	190	341	79	0.23	0.14
1_126 cm	#5	740	230	375	107	0.29	0.00
1_151 cm	#6-7	550	120	350	94	0.27	0.21
9_86 cm	#3	510	190	331	87	0.26	0.36
9_119 cm	#5	480	160	278	65	0.23	0.00
9_128 cm	#6-7	400	100	275	68	0.25	0.10
12_54 cm	#3	430	150	245	68	0.28	0.10
12_82 cm	#5	420	100	229	69	0.30	0.15
12_91 cm	#6-7	490	90	231	69	0.30	0.00

Table 7. Sand grain size and shell fragment frequency Tsunami sand layer samples are from three core sites (MOOR1, MOOR9 and MOOR12 in the Moore Creek runup locality. Population characteristics including maximum sand size (Max), minimum sand size (Min), average (mean), 1 standard deviation (Std Dev), and mean normalized standard deviation (MeanNStdDev) (Folk, 1980) are based on 50 grain counts. Carbonate shell fragment frequency (Shell frag %) are based on 1,000 grain counts. Core sites and sample intervals are shown in Fig. 5 and Fig. 7, respectively.

Carbonate shell fragments were identified in the gravel size fractions of target paleotsunami sand sheets in 7 out of the 8 runup localities (Fig. 4). Shell fragments were found in 9 of the 12 sand sheet samples that contained minor abundances of granules (size range 2-5 mm diameter). The granule abundance abruptly decreases to trace levels with increasing distance from the beach (200-400 m) and with increasing elevation (8–12 m) in the Moore Creek locality. Petrographic microscopy of the carbonate grains in the sand fractions of the target paleotsunami sand sheets in the Moore Creek locality are shown in Table 7. Though not as distinctive as the larger shell fragments, the trace abundances of the carbonate sand-size grains in representative tsunami sand layers from core sites MOOR1, MOOR9, and MOOR12, confirm that the thin sand layers were derived from littoral or inner-shelf sediment sources. Other investigators have examined mollusan shells in paleotsunami deposits (Fujiwara et al., 2003) and have recently reported the presence of foraminfera tests in tsunami deposits from the Sumatra 2004 tsunami (Hawkes et al., 2007). The use of foraminfera was not tested in this study, but it could provide a complimentary technique to the use of carbonate shell fragments, as reported here.

4.4 Grain size

The sand grain size distributions from representative samples of tsunami sand layers in the Moore Creek locality demonstrate landward fining trends (Table 7). Population means of the sand grain samples decrease from 341–375 μm in the seaward site MOOR1 to 229-245 μm in the landward site MOOR12. The apparent differences between the sand population means from the seaward and landward core sites are statistically different at the 95% confidence intervals. Both the separation in distance (~ 350 m) and elevation (4 m) between the seaward and landward sites are thought to contribute to the small, but significant, landward fining of the mean sand size.

4.5 Runup elevations

Paleotsunami deposit elevations are taken from core site surface elevations and corresponding subsurface depths of tsunami deposits (Table 8**)**. There is a close correspondence between core site surface elevations as surveyed into registered benchmarks and as estimated by GPS located sites on the LIDAR digital elevation model (U. S. Geological Survey, 2011). For the runup elevation measurements shown here we use the benchmark survey elevation control (± 5 cm elevation accuracy) in all but 3 core sites. Elevation based on LIDAR is used for core sites MOOR13-MOOR15. Terminal sand sheet elevations reach 11–12 m NAVD88 in core sites MOOR12 and MOOR13.

The measured deposit elevations in the Moore Creek locality are corrected for paleo-sea level runup height based on the age of the paleotsunami event (Table 1) and an assumed net rate of sea level rise (1.0 m per 1000 years) for the study area during late Holocene time (Darienzo et al., 1994). Paleotsunami runup heights that are corrected for net sea level rise reach 13–15 m for tsunami events #3, #5 and #6 in the Moore Creek locality. It is assumed that the terminal sand sheet proxies for runup height underestimate actual flooding elevations. However, the apparent pinchouts of the corresponding paleotsunami debris layers near core site MOOR15 suggest that maximum recorded paleotsunami runup height is closely approximated by the terminal sand sheet deposits in the Moore Creek locality.

5. Discussion

5.1 Landward trends of paleotsunami deposits in proximal settings

Several parameters including tsunami deposit sand: silt ratio, sand layer thickness, and abundance of coarse grained shell fragments are found to substantially decrease with elevation gain (from 8 m to 12 m) over the short inundation distance of 450 m in the Moore Creek locality (Fig. 7). A small, but statistically significant, decrease of mean sand size is also documented in the paleotsunami sand layers in the Moore Creek cores sites (Table 7). We attribute these landward trends to decreases in tsunami flow velocity and turbulence with lansdward increases in floodplain elevation (Fig. 8). Terminal sand sheet layers are on the order of only a few centimeters in thickness, requiring extensive coring to recover tsunami sand layers from the bioturbated floodplain deposits.

5.2 Event runup heights

A total of three sand sheets that reach 11-12 m elevation are recorded during the last 3.2 ka in the Moore Creek locality (Fig. 8). The last two events (#5 and # 6) are attributed to large magnitude runups in other central Cascadia tidal basins, back-barrier wetlands, and beach plains (Peterson et al., 2010a; Peterson et al., 2010b; Schlichting, 2000). These two paleotsunami are correlated to long inundation events in the adjacent Beaver Creek floodplain (see Section 5.3 below). When adjusted for Paleo-sea level at the time of inundation (Table 8) the three paleotsunami sand sheets reach 13-14 m runup height at the landward side of the Moore Creek runup locality. Three of the 6–7 nearfield tsunami produced by ruptures of the central Cascadia megathrust during the last 3.2 ka yielded large runup elevations in the study area. These runups would have reached 15 m above the current O m NAVD88 datum. The remaining 3–4 paleotsunami exceeded 5 m runup height, as shown by tsunami deposits at the BEAV_D1 core site in the Beaver Creek locality (Fig. 4). These smaller magnitude tsunami did not leave sand sheet deposits above 9 m elevation in Moore Creek locality (Fig. 7). We assume that their maximum runup heights did not exceed 10 m elevation at the Moore Creek runup locality.

Core Site	Core top elev. (m)	Overland distance (m)	Tsunami deposit event #	Core depth (m)	Deposit elev. (m) NAVD88	Paleo-sea level (m)	Paleo-runup height (m)
1	7.98/8.0	10	# 3 TSL	1.00	6.98	-1.0	8.0
			# 5 TSL	1.26	6.72	-2.5	9.2
			#6-7 TSL	1.54	6.44	-3.0	9.4
2	8.14/8.2	20	#3 TSL	0.83	7.31	-1.0	8.3
			#5 TSL	1.00	7.14	-2.5	9.6
			#6-7 TSL	1.38	6.76	-3.0	9.8
3	8.29/8.2	90	#3 TSL	0.55	7.74	-1.0	8.7
			TDL ?	1.00	7.29	-2.0	9.3
			#5 TSL	1.15	7.14	-2.5	9.6
			#6-7 TSL	1.53	6.76	-3.0	9.8
4/5	8.40/8.4	130	#3 TSL	0.39	8.01	-1.0	9.0
			TDL ?	0.68	7.72	-2.0	9.7
			#5 TSL	0.91	7.49	-2.5	10.0
			#6-7 TSL	1.22	7.18	-3.0	10.2
8	9.33/9.5	180	#3 TSL	0.79	8.54	-1.0	9.5
			#5 TSL	1.66	7.76	-2.5	10.3
			#6-7 TSL	1.74	7.59	-3.0	10.6
9	9.69/9.7	180	#3 TSL	0.86	8.83	-1.0	9.8
			#5 TSL	1.19	8.50	-2.5	11.0
			#6-7 TSL	1.28	8.41	-3.0	11.4
10	10.57/11.9	270	#3 TSL	0.50	10.07	-1.0	11.1
			#5 TSL	0.78	9.79	-2.5	12.3
			#6-7 TSL	1.02	9.55	-3.0	12.5
11	10.52/10.6	280	#3 TSL	0.69	9.83	-1.0	10.8
			#5 TSL	0.98	9.54	-2.5	12.0
12	12.17/13.3	400	#3 TSL	0.54	11.63	-1.0	12.6
			#5 TSL	0.82	11.35	-2.5	13.8
			#6-7 TSL	0.91	11.26	-3.0	14.3
13	na/12.8	450	#3 TSL	0.51	12.3	-1.0	13.3
			#5 TSL	0.79	12.0	-2.5	14.5
			#6-7 TDL	0.98	11.8	-3.0	14.8
14	na/13.0	450	#3 TDL	0.4	12.6	-1.0	13.6
			#5 TDL	0.97	12.0	-2.5	14.5
15	na/13.2	540	#3 TDL ?	0.5	12.7	-1.0	13.7
			#5 TDL ?	0.85	12.3	-2.5	14.8

Table 8. Core site and paleotsunami deposit elevations in the Moore Creek locality. Core site data: core top elevation from total station survey to registered benchmark/LIDAR (m) NAVD88 and overland inundation flow distance (m) from the shoreline. Tsunami deposit: event number (#), depth in core (m) and computed elevation relative to NAVD88 datum. Paleo-sea level estimated for event ages #3 (~ 1.3 ka), #5 (~ 2.6 ka), #6 (~ 2.8 ka), and # 7(~ 3.2 ka) assuming 1 m/1000 year relative sea level rise. Tsunami runup height (m) equivalent to NAVD88 datum but adjusted for lower paleo-sea level at the time of inundation. See Fig. 5 for core site locations.

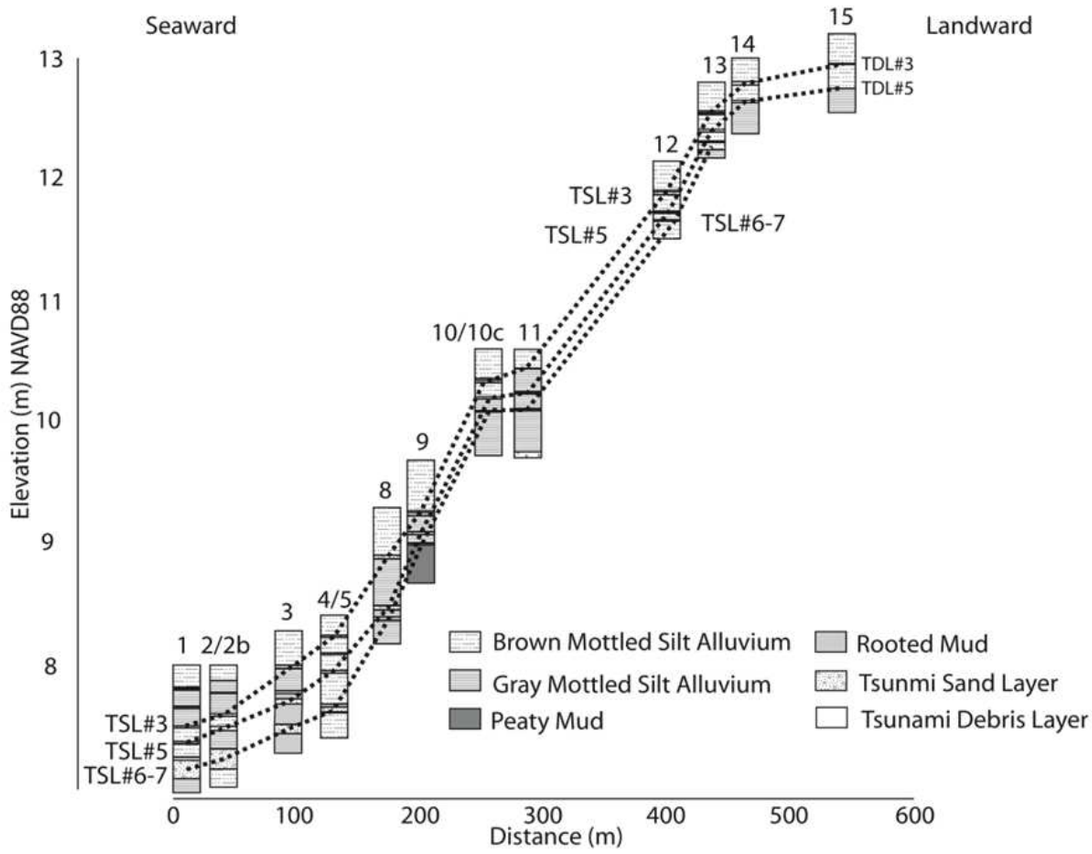

Fig. 8. Topographically corrected cross-section of stratigraphically correlated paleotsunami deposits (dotted lines) for events #3, #5, and #6–7 in the Moore Creek floodplain. Tsunami sand layers (TSL) pinchout to tsunami debris layers (TDL) with increasing distance and elevation from the present beach–terrace edge. Vertical exaggeration is ~ 100x. See Fig. 5 for core site locations.

5.3 Landward runup height attenuation in Beaver Creek

Using the maximum-recorded extents of tsunami sand sheet deposition as proxies for paleotsunami runup in Moore Creek and Beaver Creek (Fig. 2) we establish a runup height attenuation gradient for paleotsunami event #3 in the study area. Differences between paleotsunami event #3 sand layer elevations and runup distances in the proximal core site MOOR13 (12.3 m elevation at 0.45 km distance) (Table 8) and the distal core site BEAV03 (1.2 m elevation at 3.7 km distance) (Peterson et al., 2010a) yield an attenuation gradient of 3.4 m km^{-1} (Fig. 9). Using the attenuation gradient we extrapolate a shoreline runup elevation of 13.8 m at 0 m distance. Adjusting for Paleo-sea level (-1.0 m) at 1.3 ka we predict a runup height of 14.8 m based on paleotsunami sand sheet deposition. This extrapolated sand deposition height might underestimate actual surge height at the shoreline.

5.4 Test of runup height attenuation gradient at Cannon Beach

The landward gradient of runup attenuation is tested in another central Cascadia locality, Cannon Beach, Oregon (Fig. 1), which was previously surveyed for distal and proximal

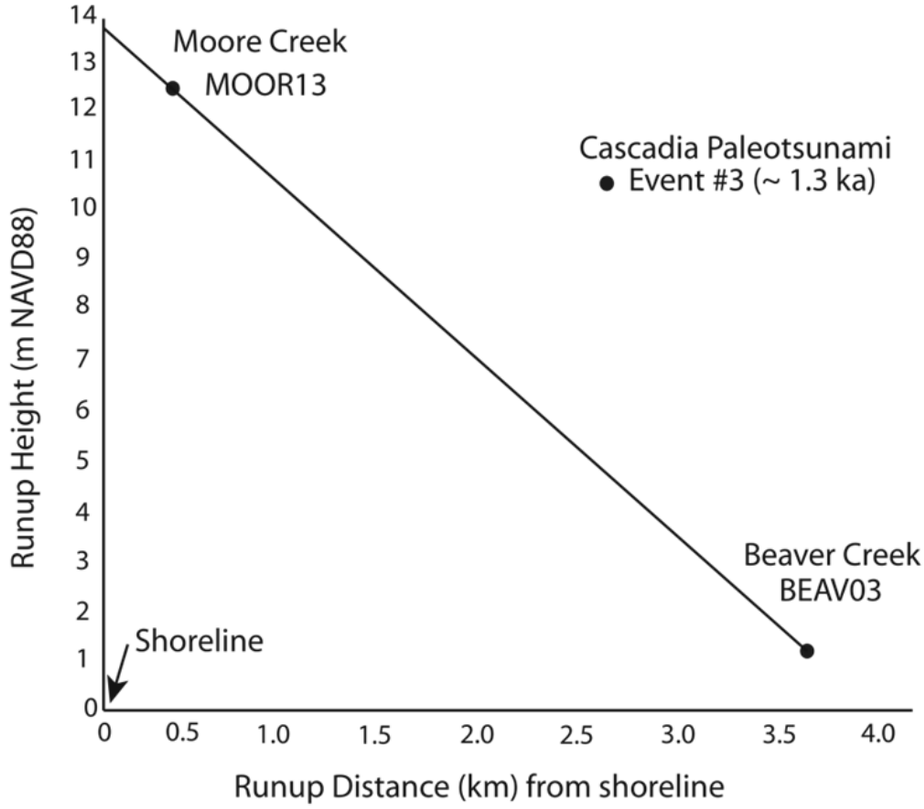

Fig. 9. Runup attenuation for the #3 paleotsunami event in Moore Creek and Beaver Creek in the study area. The position and elevation of terminal sand sheet deposition are from Table 8 in Moore Creek and from (Peterson et al. (2010a)) in Beaver Creek. The proximal runup site (MOOR13) represents terminal sand sheet deposition in a high-gradient creek floodplain perched on a seaward facing hillslope. The distal site (BEAV03) represents terminal sand sheet deposition in a low gradient floodplain developed in a broad alluvial valley.

runup records (Peterson & Cruikshank, 2007; Peterson et al., 2008). The terminal extent of paleotsunami sand sheet deposition from event #3 (~ 1.3 ka) was traced to site C72 (6.5 m elevation at 2.1 km landward distance). Using the attenuation gradient of 3.4 m km^{-1} over the runup distance of 2.1 km and the core depth corrected elevation of 6.5 m for the event #3 sand layer at site C72 (Peterson et al., 2008) a predicted shoreline runup elevation of 13.6 m is calculated for Cannon Beach (Fig. 10). The projected elevation of shoreline runup at Cannon Beach (13.6 m) is similar to that projected for the Moore Creek locality (13.8 m) at the shoreline for the paleotsunami event # 3 (Fig. 9).

Upland terrace sites in Cannon Beach lack ideal hosting deposits for recording paleotsunami deposits. However two localities in a very small gully floodplain adjacent to Coolidge Avenue in Cannon Beach (sites CANU116 and CANU119) were identified as potential runup sites based on anomalous sandy intervals (Fig. 10). CANU116 at 8.4 m elevation, and 220 m landward distance, contained two prominent quartz-rich sand layers at 14–16 and 49–51 cm depth (Fig. 11). The most landward extent of an anomalous sandy debris layer, including rounded granules, was observed at 64-67 cm depth in CANU119 at an elevation of

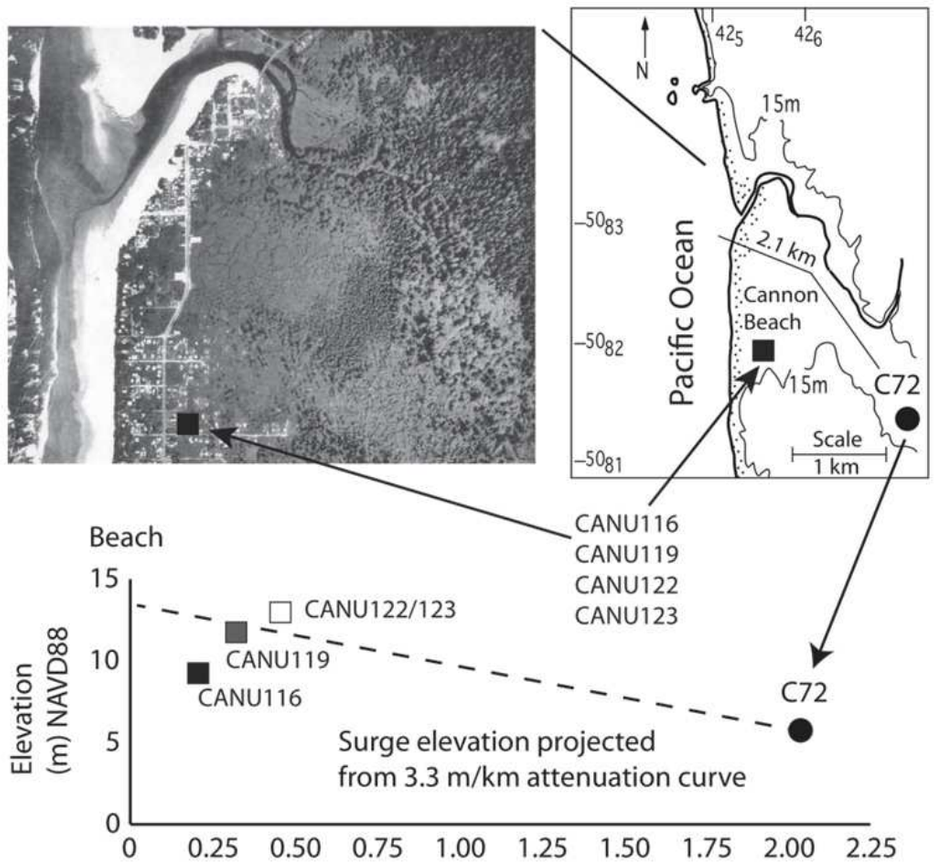

Fig. 10. Estimation of shoreline runup elevation for paleotsunami event #3 (~1.3 ka) in Cannon Beach, Oregon. Historic photograph of Cannon Beach shows Ecola Creek valley topography prior to extensive development in the middle to late 1900s. The proximal runup estimates are based on 1) terminal sand sheet deposition in core site C72 (solid circle in map inset) at 6.5 m elevation and 2.1 km flow inundation distance, and 2) reverse extrapolation of attenuation gradient 3.4 m km^{-1} (dashed line) to the shoreline (plot diagram). Adjustment for paleo-sea level yields a modern runup height of 15 m at the shoreline in Cannon Beach. Preliminary searches for possible paleotsunami sand sheets yielded two sand layers at CANU116 (UTM 5082190n 42542e) and a most landward extent of an anomalous sandy debris layer at CANU119 (UTM 5082054n 425584e) as shown in Fig. 11. No sand layer or sandy debris layers were observed at core sites CANU122 (UTM 5082134n 425662e) or CANU123 (UTM 5082078n 425654e). See Fig. 1 for the location of Cannon Beach in the central Cascadia margin.

11.3 m and a landward distance of 300 m. No sand layers were observed at CANU122 at 12.7 m elevation, or CANU1213 at 13.5 m, both at a distance of 440 m from the beach. The anomalous sandy layers at CANU116 and CANU119 were not radiocarbon dated at the time of the reconnaissance survey (2006) due, in part, to a lack of target runup elevations. Such target elevations are now provided by the projected runups from the attenuation gradient shown in Fig. 10.

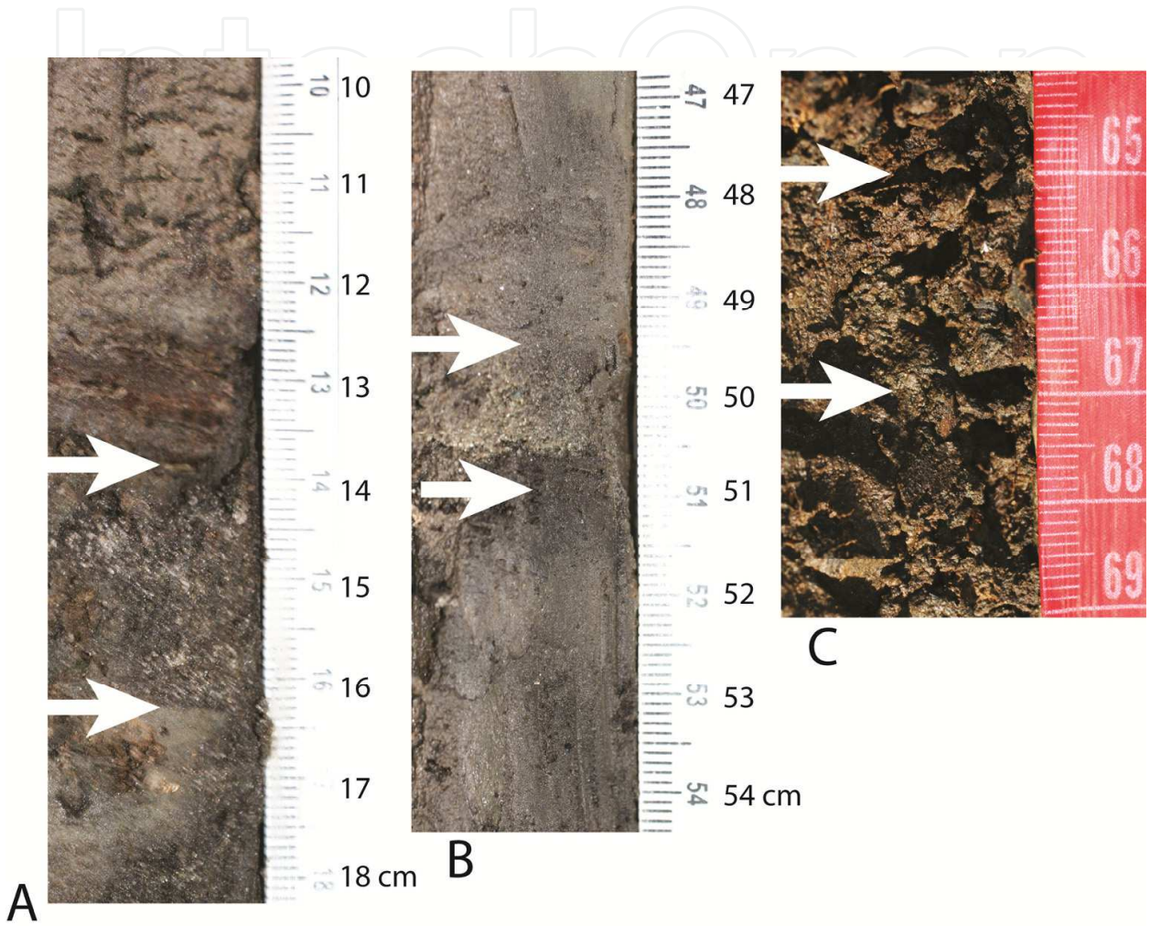

Fig. 11. Photos of target paleotsunami sand layers from CANU116 at 14-16 cm depth (photo A), CANU116 at 49-51 cm depth (photo B), and CANU119 at 64-67 cm depth (photo C). A detrital wood fragment at 13 cm depth overlies the upper sand layer in CANU116 (photo A). The lower sand layer in CANU116 shows a sharp bottom contact and fining-upward sand grain size, both features are characteristic of paleotsunami deposits. The sandy debris layer at 64-67 cm depth in CANU119 includes rounded granules, well above wind-blown grain size thresholds. All three layers contain rounded quartz grains (beach sand source mineralogy) but the target paleotsunami sand layers from CANU116 have yet to be radiocarbon dated.

6. Conclusion

Small creek floodplains (< 500 m from the shoreline and > 6-7 m elevation) provide stable hosting settings for recording prehistoric tsunami inundation events in the central Cascadia subduction zone. The floodplain silts extend back to 3–4 ka in time, permitting the potential geologic recording of anomalous sand sheets from 6–7 nearfield tsunami during that time interval. A total of 3-4 paleotsunami deposits exceed 8 m in elevation, and 3 paleotsunami sand sheets can be traced to 12 m elevation. Adjusting for Paleo-sea level at the time of inundation the estimated runup for the 3 paleotsunami at the shoreline is 15 m in height. Minimum runups for nearfield tsunami in the study area are greater than 5 m height, based on the geologic record of smaller scale tsunami in a creek setting with a low-threshold elevation (~ 4.5 m) for inundation. The measured runup heights for central Cascadia paleotsunami during the last 3.2 ka are 10+/- 5 m. An attenuation gradient of 3.4 m km^{-1} is estimated from terminal sand sheet deposition produced by the last large runup event (at ~ 1.3 ka) as recorded in both proximal and distal floodplain settings in the study area. The attenuation gradient permits an extrapolation of distal terminal runup records to yield estimated shoreline runup heights for this tsunami event in other similar floodplain localities in the central Cascadia margin. The prehistoric runup records can be used to test and/or calibrate numerically modeled tsunami hazard in the region. The methodology used here should have broad use in other susceptible coastlines that have not experienced catastrophic tsunami inundation in historic time.

7. Acknowledgments

Roger Hart assisted with the first paleotsunami investigations in the Henderson creek floodplains in the study area. We dedicate this paper to Roger Hart (1940-2011) for his spirit of scientific exploration.

Robert Schlichting preformed the diatom analysis for this study. Anna Pilette assisted with detailed core logging, sampling, and photography of the Grant and Moore Creek tsunami sand sheets. Preliminary surveying of study area floodplains for target paleotsunami deposit included assistance from Steve Ahlquist, Andrea Adair, Tim Blazina, Adam Cambell, Charles Cannon, Annie Donehey, Brandon Ezzell, Ben Freudenberg, Christopher French, Jonathan Huster, Audra Inglish, Jenifer Lind, Robert Linscott, Fiona Seifert, Andrew Shaddox, Liza Shaw, Scott Waibel, Rex Whistler. Georg Grathoff and Karen Carroll provided XRD analyses of granule mineralogy from the Theil Creek paleotsunami deposits. David Percy provided assistance with LiDAR topographic imaging and elevation control of core sites. Meredith Savage and Derrick Tokos provided assistance with Newport City topographic interpretations. Stewart Cowy provided assistance with Lincoln County topographic flood maps and with interpretations of historic development features. The Oregon Department of Geology and Mineral Industries provided funding for field travel during the early phase of the creek floodplain surveys. The Office of Research at Portland State University provided some support for radiocarbon dating. LiDAR data was provided through USGS National Elevation Dataset (NED) with technical assistance from Sheri Schneider.

8. References

Atwater, B. F., Nelson, A. R., Clague, J. J., Carver, G. A., Yamaguchi, D. K., Bobrowsky, P. T., Bourgeois, J., Darienzo, M. E., Grant, W. C., Hemphill-Haley, E., Kelsey, H. M., Jacoby, G. C., Nishenko, S. P., Palmer, S. P., Peterson, C. D., and Reinhart, M. A. (1995), Summary of coastal geologic evidence of past great earthquakes at the Cascadia subduction zone: *Earthquake Spectra*, Vol. 11, No. 1, pp. 1-18.

Atwater, B. F., Tuttle, M. P., Schweig, E. S., Rubin, C. M., Yamaguchi, D. K., and Hemphill-Halley, I. (2004), Earthquake recurrence, inferred from paleoseismology, In: *The Quaternary Period in the United States*, Gillespie, A. R., Porter, S. C., and Atwater, B. F., Amsterdam, Elsevier, p. 331-350.

Carver, G. A., Abramson, H. A., Garrison-Laney, C. E., and Leroy, T. (1998), Investigation of paleotsunami evidence along the north-coast of California, Pacific Gas and Electric Company, p. 167.

Clague, J. J., Bobrowsky, P. T., and Hutchinson, I. (2000), A review of geologic records of large tsunami at Vancouver Island, British Columbia, and implications for hazard: *Quaternary Science Reviews*, Vol. 19, No., pp. 849-863.

Cruikshank, K. M., and Peterson, C. D. (2011), Oregon Tsunami Database, Geology Department, Portland State University, http://geomechanics.geology.pdx.edu/geolinq/tsunami

Darienzo, M. E., Peterson, C. D., and Clough, C. (1994), Stratigraphic evidence for great subduction zone earthquakes at four estuaries in Northern Oregon: *Journal of Coastal Research*, Vol. 10, No. 4, pp. 850-876.

Dengler, L. A. (2006), Awareness and Preparedness, In: *Summary Report on the Great Sumatra Earthquakes and Indian Ocean Tsunamis of 26 December 2004 and 28 March 2005*, Oakland, CA, Earthquake Engineering Research Institute, p. 51-65.

Folk, R. L. (1980), *Petrology of sedimentary rocks*: Austin, Texas, Hemphill Publishing Co., 188 p.

Fujiwara, O., Kamataki, T., Fuse, K., and Daiyonki, K. (2003), Genesis of mixed molluscan assemblages in the tsunami deposits distributed in Holocene drowned valleys on the southern Kanto region, east Japan: *Quaternary Research*, Vol. 42, No., pp. 389-412.

González, F. I., Geist, E. L., Jaffe, B., Kânoğlu, U., Mofjeld, H., Synolakis, C. E., Titov, V. V., Arcas, D., Bellomo, D., Carlton, D., Horning, T., Johnson, J., Newman, J., Parsons, T., Peters, R., Peterson, C. D., Priest, G., Venturato, A., Weber, J., Wong, F., and Yalciner, A. (2009), Probabilistic tsunami hazard assessment at Seaside, Oregon, for near- and far-field seismic sources: *Journal of Geophysical Research*, Vol. 114, No., pp. C11023, doi:10.1029/2008JC005132.

Google (2011), Google Earth, Mountain View, CA, Google, http://www.google.com/earth/index.html.

Hart, R., and Peterson, C. D. (2007), Late-Holocene buried forests on the Oregon coast: *Earth Surface Processes and Landforms*, Vol. 32, No. 2, pp. 210-229, doi:10.1002/esp.1393.

Hawkes, A. D., Bird, M., Cowie, S., Grundy-Warr, C., Horton, B. P., Hwai, A. T. S., Law, L., Macgregor, C., Nott, J., Ong, J. E., Rigg, J., Robinson, R., Tan-Mullins, M., Sa, T. T., Yasin, Z., and Aik, L. W. (2007), Sediments deposited by the 2004 Indian Ocean Tsunami along the Malaysia-Thailand Peninsula: *Marine Geology*, Vol. 242, No., pp. 169-190, doi:10.1016/j.margeo.2007.02.01.

Hemphill-Haley, E. (1996), Diatoms as an Aid in Identifying late-Holocene Tsunami Deposits: *The Holocene*, Vol. 6, No. 4, pp. 439-448.

Hutchinson, I., Clague, J., and Mathewes, R. W. (1997), Reconstructing the tsunami record on an emerging coast: A case study of Kanim Lake, Vancouver Island, British Columbia, Canada: *Journal of Coastal Research*, Vol. 13, No., pp. 545-553.

Kelsey, H. M., Nelson, A. R., Hemphill-Haley, E., and Witter, R. C. (2005), Tsunami history of an Oregon coastal lake reveals a 4600 yr record of great earthquakes in the Cascadia subduction zone: *Geological Society of America Bulletin*, Vol. 117, No. 7/8, pp. 1009-1032, doi:10.1130/B25452.1.

Peterson, C. D., Chadha, R. K., Cruikshank, K. M., Francis, M., Latha, G., Katada, T., Singh, J. P., and Yeh, H. (2006), Preliminary comparison of December 26, 2004 Tsunami records from SE India and SW Thailand to paleotsunami records of overtopping height and inundation distance from the central Cascadia margin, USA: NCEE 8th Annual Proceedings, p. Paper 8.

Peterson, C. D., and Cruikshank, K. M. (2007), Tsunami database description for geologic records of overland paleotsunami inundation at Cannon Beach and at selected localities in Lincoln County, Oregon, Final Report on Oregon tsunami database for Department of Oregon Geology and Mineral Industries, Portland, OR, Department of Geology, Portland State University, p. 27.

Peterson, C. D., Cruikshank, K. M., Jol, H. M., and Schlichting, R. B. (2008), Minimum runup heights of paleotsunami from evidence of sand ridge overtopping at Cannon Beach, Oregon, Central Cascadia Margin, USA: *Journal of Sedimentary Research*, Vol. 78, No., pp. 390-409, doi:10.2110/jsr.2008.044.

Peterson, C. D., Cruikshank, K. M., Schlichting, R., and Braunsten, S. (2010a), Distal Runup Records Of Latest Holocene Paleotsunami Inundation In Alluvial Flood Plains: Neskowin and Beaver Creek, Oregon, Central Cascadia Margin, USA: *Journal of Coastal Research*, Vol. 26, No., pp. 622-634, doi:10.2112/08-1147.1.

Peterson, C. D., Jol, H. M., Horning, T., and Cruikshank, K. M. (2010b), Paleotsunami Inundation of a Beach Ridge Plain: Cobble Ridge Overtopping and Inter-ridge Valley Flooding in Seaside, Oregon, USA: *Journal of Geologic Research*, Vol. 2010, No. 276989, pp. 22, doi:10.1155/2010/276989.

Schlichting, R. B. 2000, Establishing the inundation distance and overtopping height of paleotsunami from late-Holocene geologic records at open-coastal wetland sites, central Cascadia margin: Unpub. MS Thesis thesis, Portland State University 166 p.

Schlichting, R. B., and Peterson, C. D. (2006), Mapped overland distance of paleotsunami high-velocity inundation in back-barrier wetlands of the central Cascadia margin, U.S.A.: *Journal of Geology*, Vol. 114, No. 5, pp. 577-592.

U. S. Geological Survey (2011), Seamless Data Warehouse, NED1/9ArcSec, U S Geological Survey, http://seamless.usgs.gov/ned19.php.

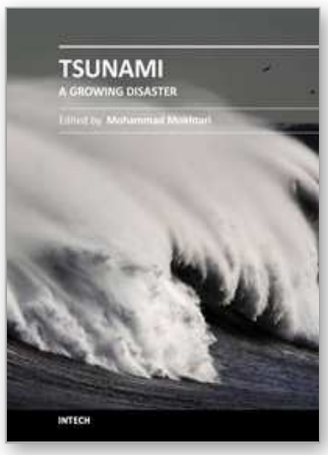

Tsunami - A Growing Disaster
Edited by Prof. Mohammad Mokhtari

ISBN 978-953-307-431-3
Hard cover, 232 pages
Publisher InTech
Published online 16, December, 2011
Published in print edition December, 2011

The objective of this multi-disciplinary book is to provide a collection of expert writing on different aspects of pre- and post- tsunami developments and management techniques. It is intended to be distributed within the scientific community and among the decision makers for tsunami risk reduction. The presented chapters have been thoroughly reviewed and accepted for publication. It presents advanced methods for tsunami measurement using Ocean-bottom pressure sensor, kinematic GPS buoy, satellite altimetry, Paleotsunami, Ionospheric sounding, early warning system, and scenario based numerical modeling. It continues to present case studies from the Northern Caribbean, Makran region and Tamil Nadu coast in India. Furthermore, classifying tsunamis into local, regional and global, their possible impact on the region and its immediate vicinity is highlighted. It also includes the effects of tsunami hazard on the coastal environment and infrastructure (structures, lifelines, water resources, bridges, dykes, etc.); and finally the need for emergency medical response preparedness and the prevention of psychological consequences of the affected survivors has been discussed.

InTech Europe
University Campus STeP Ri
Slavka Krautzeka 83/A
51000 Rijeka, Croatia
Phone: +385 (51) 770 447
Fax: +385 (51) 686 166
www.intechopen.com

InTech China
Unit 405, Office Block, Hotel Equatorial Shanghai
No.65, Yan An Road (West), Shanghai, 200040, China
中国上海市延安西路65号上海国际贵都大饭店办公楼405单元
Phone: +86-21-62489820
Fax: +86-21-62489821

IntechOpen